EU EDF – SOPAC Project Report 135
Reducing Vulnerability of Pacific ACP States

TONGA TECHNICAL REPORT

Hydrodynamic Model of Fanga'uta lagoon: Water Circulation and Applications

October 2008

Prepared by:
Herve Damlamian
SOPAC Secretariat
September 2008

PACIFIC ISLANDS APPLIED GEOSCIENCE COMMISSION
c/o SOPAC Secretariat
Private Mail Bag
GPO, Suva
FIJI ISLANDS
http://www.sopac.org
Phone: +679 338 1377
Fax: +679 337 0040
www.sopac.org
director@sopac.org

Important Notice

This report has been produced with the financial assistance of the European Community; however, the views expressed herein must never be taken to reflect the official opinion of the European Community.

TABLE OF CONTENTS

LIST OF FIGURES

LIST OF TABLES

Acknowledgements

- To Dr Arthur Webb, Aggregate Management Adviser of the SOPAC/EU project, for his advice leading to good water quality fieldwork.
- To Franck Magron, Reef Fisheries Information anager at SPC, for extracting the bathymetry of Tongatapu from satellite imagery.
- To the Ministry of Mineral Resources and Ministry of Environment of Tonga for assisting with the fieldwork in Fanga'uta lagoon.

Malo!

EXECUTIVE SUMMARY

Damlamian, H. 2008: Hydrodynamic Model of Fanga'uta lagoon, Tonga: Water Circulation and Applications. *EU EDF 8 – SOPAC Project Report 135*. Pacific Islands Applied Geoscience Commission: Suva, Fiji, iv + 22 p.

With the development of powerful computers, numerical models are increasingly being used to simulate processes of nature. Mike21 is one example of professional modeling software for two-dimensional free surface flows; it comes in modular form with four main application areas: coastal hydraulics and oceanography, waves, sediment processes and environmental hydraulics.

This work was undertaken as part of the SOPAC/EU project EDF8, aiming to create a realistic numerical model of Fanga'uta lagoon and understand its water circulation. The numerical model, used as a management tool, could offer a sustainable way to address any future coastal management project related to Fanga'uta lagoon. This model could be further developed to provide a baseline for study of water quality scenarios, dredging impact, sediment transport, etc.

The Secretariat of the Pacific Community (SPC) requested from SOPAC information on the hydrodynamic in Tongatapu lagoon, to better understand the distribution and recruitment pattern of trochus shells. Using available data, understanding of the overall water circulation of Tongatapu lagoon was arrived at (discussed in an appendix to this report.

Current can be generated by tide, wind and waves. Their relative importance proved different for both regions, Fanga'uta and Tongatapu lagoon.

Fanga'uta lagoon is enclosed with a unique shallow entrance: only the tide generates a significant current in its vicinity. By contrast, Tongatapu lagoon is widely open to the ocean. Its water circulation is complex as tide-, wind- and wave-induced currents have a significant role to play.

Acoustic Doppler Profiler (ADP) and Acoustic Doppler Velocity (ADV) current meters were deployed in Fanga'uta lagoon but failed to properly record data. However, the model could be developed from older data.

Four distinct circulation pattern were identified using the model, highlighting the dominancy of the tide-induced current. Two dominant patterns show the classical flood and ebb current clearly to flush in and flush out the lagoon. Also, the three-dimensional shape of the Fanga'uta lagoon induces two interesting secondary patterns, were the eastern and western branches of the lagoon are connected. The volume of water exchange between the two branches over a tidal cycle is estimated to be 15.4 million cubic metres.

Tidal lag between Pea, Vaini and Nuku'alofa wharf was also analysed. Pea, being connected to the lagoon entrance via a narrow and sinuous channel, has a maximum tidal lag of almost four hours.

Renewal time was calculated showing Pea to be the most vulnerable area of the lagoon in case of a pollution scenario, with a renewal time longer than 7 days. Renewal time for the entire Fanga'uta lagoon was estimated to be around 30 days.

1. INTRODUCTION

Harbours and lagoons are all subject to some, or all, of the following disturbances: pollution, wave action, storm surge, tsunami, erosion and sedimentation, and sea-level rise. But studies linked to coastal management are often limited by the data sets available, seasonal variations and cost.

Numerical modeling provides an opportunity to view and analyse coastal problems and risks. It allows a valuable symbiosis between development and application with minimal penalties for error.

The production of a hydrodynamic model of Fanga'uta lagoon using MIKE21 software was undertaken using several sources of bathymetry data such as multibeam bathymetry data, singlebeam bathymetry data, derived bathymetry extracted from LANDSAT and marine chart data.

Fanga'uta lagoon is a shallow and enclosed body of water, only open to the ocean via a relatively shallow entrance (<5 m). The model was used to provide information on circulation patterns and water renewal time within the lagoon.

Such basic information assists coastal or lagoon management projects, and could also be used to directly address impact related to such a project. Any scenario involving water changes, sediment transport, dredging, etc. can be accurately answered using this hydrodynamic baseline.

In anticipation of further work with this model, water quality data was collected in the Nuku'alofa branch and Pea, the western side of Fanga'uta lagoon. Its outcome is detailed in Appendix 2.

At the request of the Secretariat of the Pacific Community (SPC), the water circulation model area was extended to the entire Tongatapu lagoon. Although the data were insufficient for a rigorous hydrodynamic study, the best answer possible is provided and summarized in Appendix 1

2. PHYSICAL CHARACTERISTIC

2.1 Tongatapu and Fanga'uta Lagoon

Tongatapu is located in the Pacific Ocean, 21 degree south of the equator and 175 degrees west of Greenwich. It is the largest and the most populated island of the Kingdom of Tonga.

The south coast of Tongatapu borders the ocean whereas the north coast is facing a large lagoon of about 412 square kilometres with a mean depth of about 13 m. This lagoon is open from the north and mainly closed on the eastern and western side by two barrier reefs. The eastern reef is open from one wide and very deep channel, of about 500 m deep, called Piha passage.

Fanga'uta lagoon is a shallow embayment of about 36.6 square kilometres with a mean depth of about 1 m (standard deviation, SD = 1 m). This lagoon is open to the ocean only from one mouth facing Piha passage, being 2.5 km wide at the entrance and 1.75 km at its end, with an average depth of 1.5 m (SD = 1.15). The entrance comprises one 5-meter deep channel; the second channel is wider and shallower, through a broad expanse of reef flat exposed at low tide.

Two branches separated by a complex system of reefs compose Fanga'uta lagoon. The western part, the Nuku'alofa branch, is a wide and sinuous channel of 4.7 km long and between 0.5 and 1 km wide. Its average depth is about 1.13 m (SD = 0.7), maximum depth being about 3 m. A broad, shallow basin, Pea, surrounds Kanatea Island. Its mean depth is 0.3 m (SD = 0.2). On the other side, the Mu'a branch can be subdivided into the Vaini sector, a shallow basin and the Mu'a sector, a deeper basin leading the water in and out Vaini. Their mean depth is 0.6 m (SD = 0.5) and 2 m (SD = 1.2), respectively.

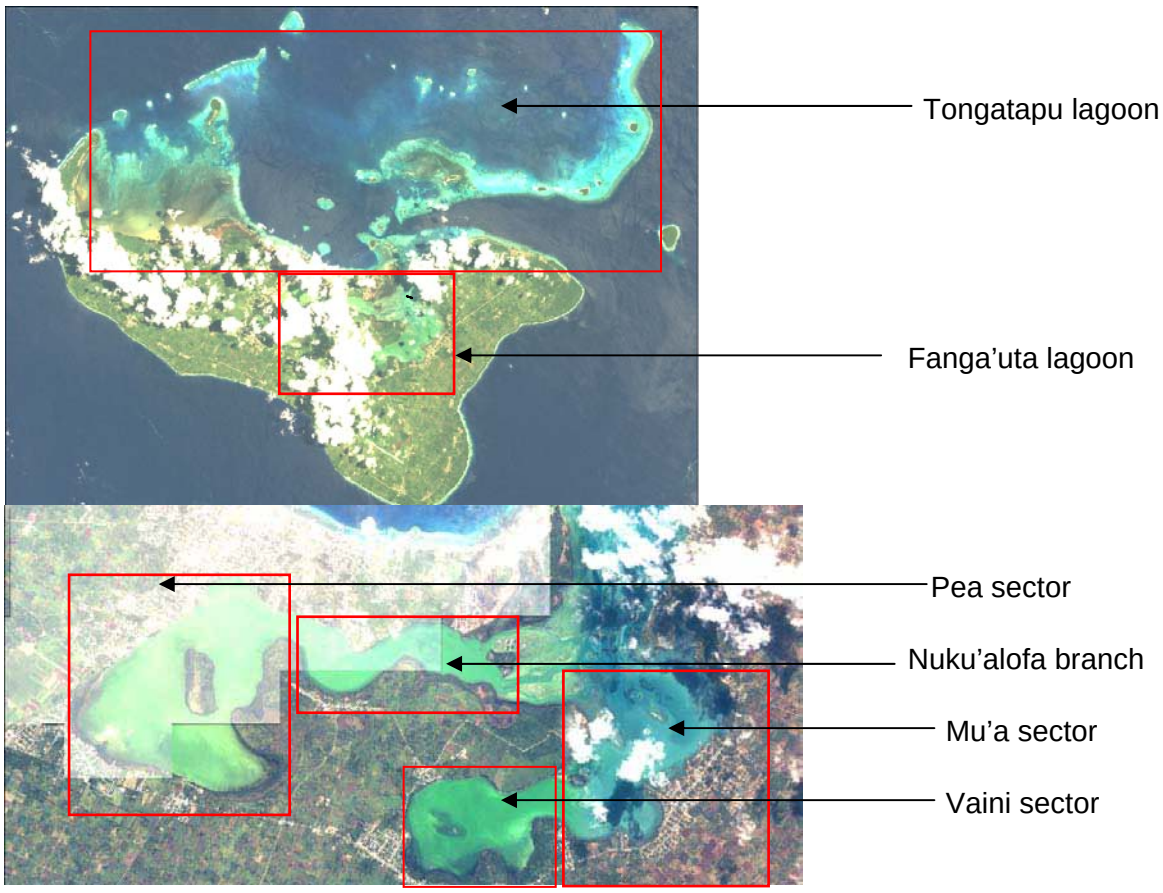

Figure 1: Tongatapu and Fanga'uta lagoon

2.2 Tides

A gauge at Nuku'alofa wharf permanently collects tidal data in the Tongatapu lagoon. This tide gauge was set up as part of the South Pacific Sea Level and Climate Project (www.pacificsealevel.org). The tides are semi-diurnal with a significant inequality between two successive highs. The tidal range varies between 1.7 m (spring) and 0.6 m (neap).

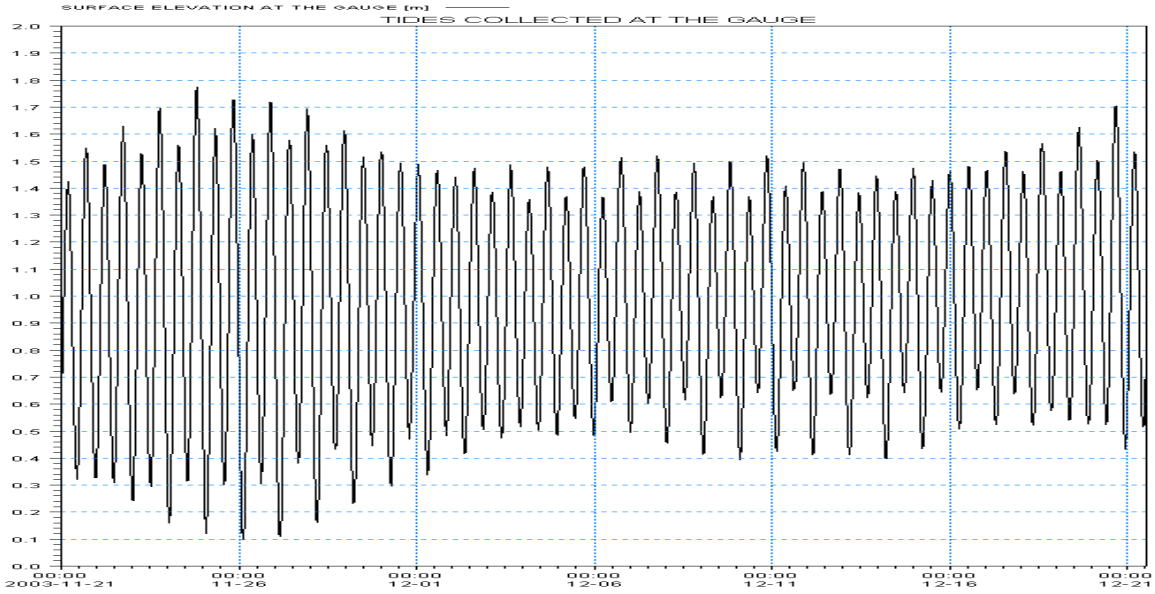

Figure 2: Tide gauge data

2.3 Winds

The wind is easterly dominant, with an annual mean direction of 130 degree. The annual mean wind speed is 4 m/s (Figure 3).

During the simulated period, the wind blows only from the east, with a mean speed of 4 m/s (Figure 4).

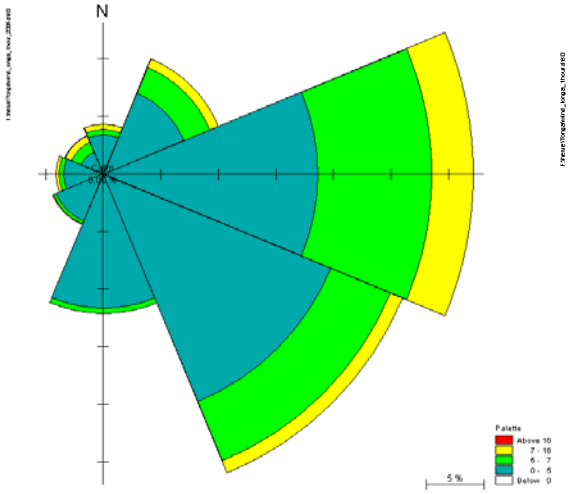

Figure 3: Annual wind rose

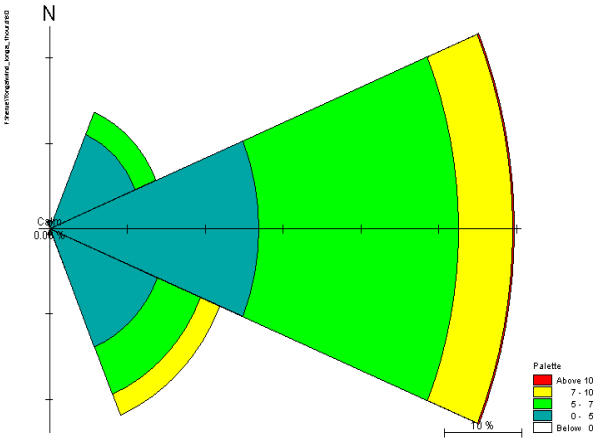

Figure 4: Wind rose during simulation

3. MODEL DESCRIPTION

3.1 Bathymetry

Several sources of data were used to create the bathymetry. SOPAC/EU undertook two bathymetry surveys in Tongatapu: one focusing on the periphery of Tongatapu, collecting multibeam data; and one in the Fanga'uta lagoon collecting singlebeam data.

Bathymetry data derived from LANDSAT imagery as well as marine chart data were used inside Tongatapu lagoon.

The offshore bathymetry data were extracted from S2004 global data. However, better resolution would be needed to draw the eastern reef bathymetry slope. As no data for this area is available, the eastern reef slope has been estimated from the adjacent data collected in Piha passage.

A flexible mesh method, using a triangular area from 250 000 m^2 to 7000 m^2 controlled the spatial accuracy, with mesh refinement performed in relation to depth.

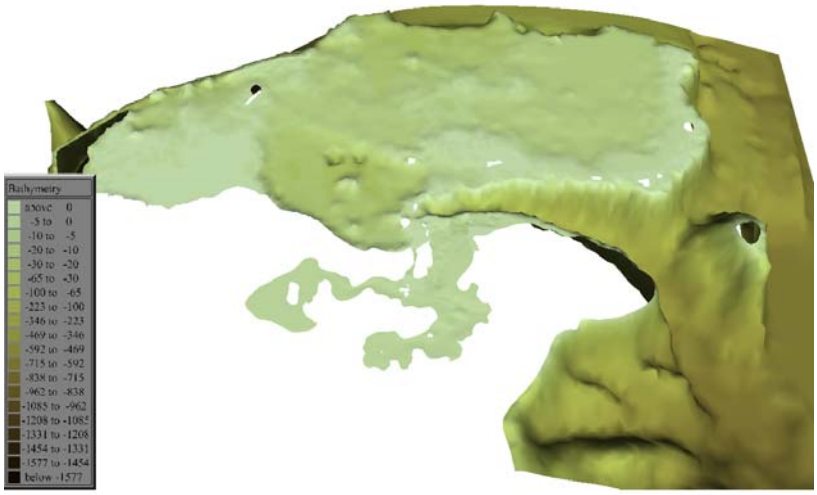

Figure 5: Bathymetry of Tongatapu lagoon

Two main parameters were used to calibrate the model: wind friction and bottom roughness.

A bottom roughness map was used to help calibrate the model. Roughness was mapped on a rectangular 100-m grid, using the Manning number.

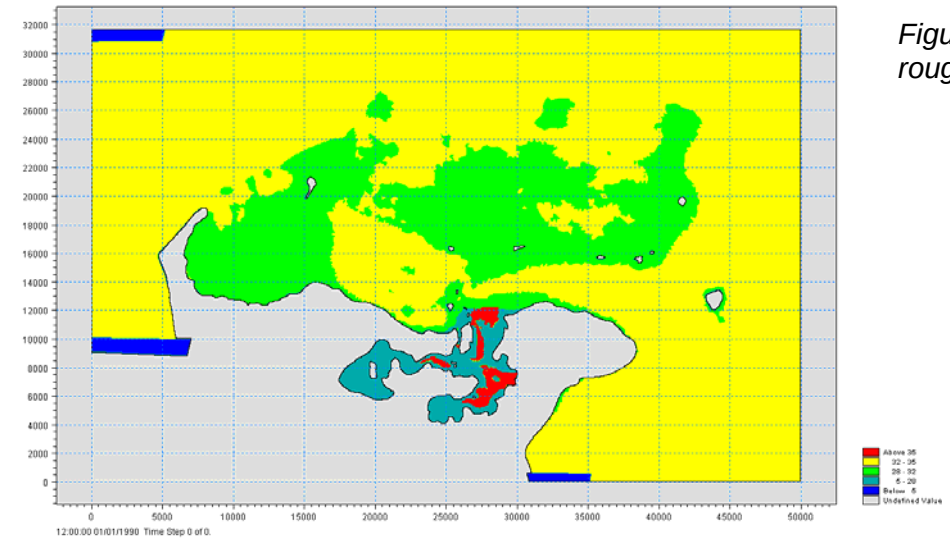

Figure 6: Map of bottom roughness

4. CALIBRATION

Acoustic Doppler Profiler (ADP) and Acoustic Doppler Velocity (ADV) current meters were deployed in Fanga'uta lagoon to collect current data in 2003 and 2006. Recorded data files from both surveys turned out to be corrupted: no rational explanation was found. Crucial data were lost, such as the current data in the entrance of Fanga'uta lagoon. Fortunately, some data could be retrieved and calibration was done as well as was possible. Results from the model are well correlated with previous hydrodynamic studies undertaken in the lagoon.

The Fanga'uta model was thus calibrated with only two sources of data: surface elevation data from the gauge in Nuku'alofa and ADV data in Fanga'uta lagoon next to the power station.

Calibration of the Tongatapu lagoon was done using ADP data collected in December 2003 in the western reef; this is detailed in Appendix 1.

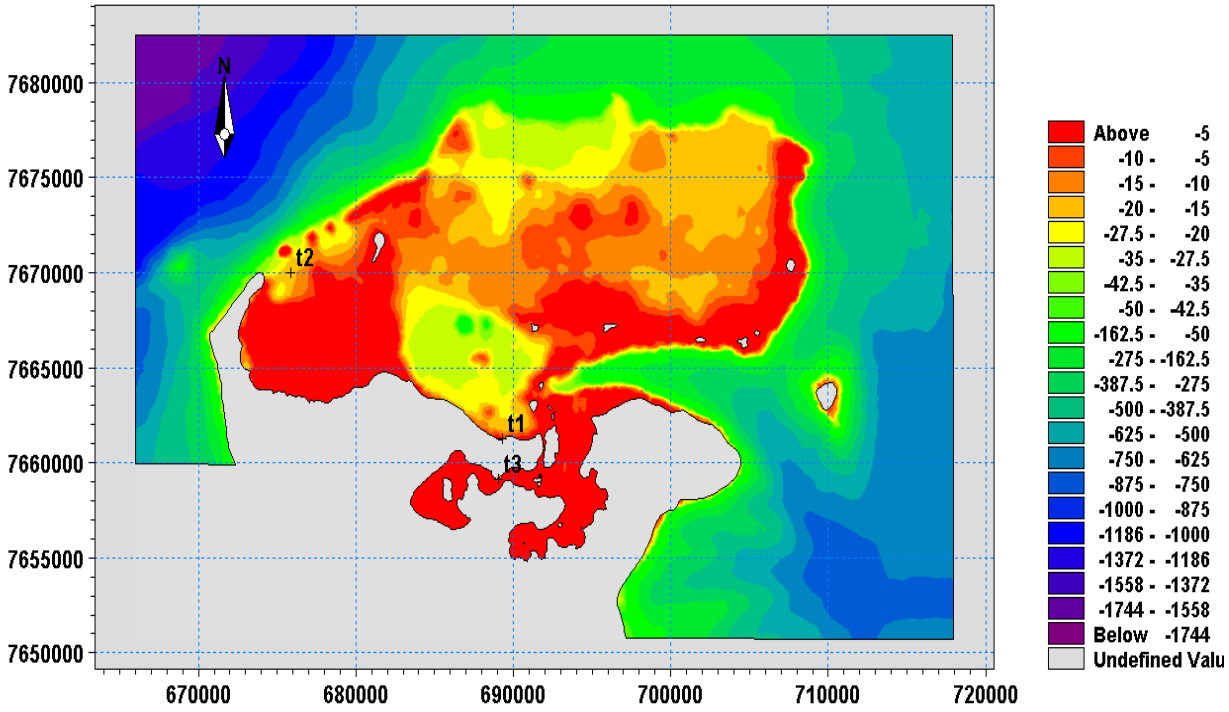

Figure 7: Tide gauge (t1) and current meter locations (t2: ADP, t3: ADV).

4.1 Surface Elevation

Figure 8 shows a comparison between the extracted data and the real data. The simulated surface elevation matches the tide gauge data very well, with a maximum error of 1 cm.

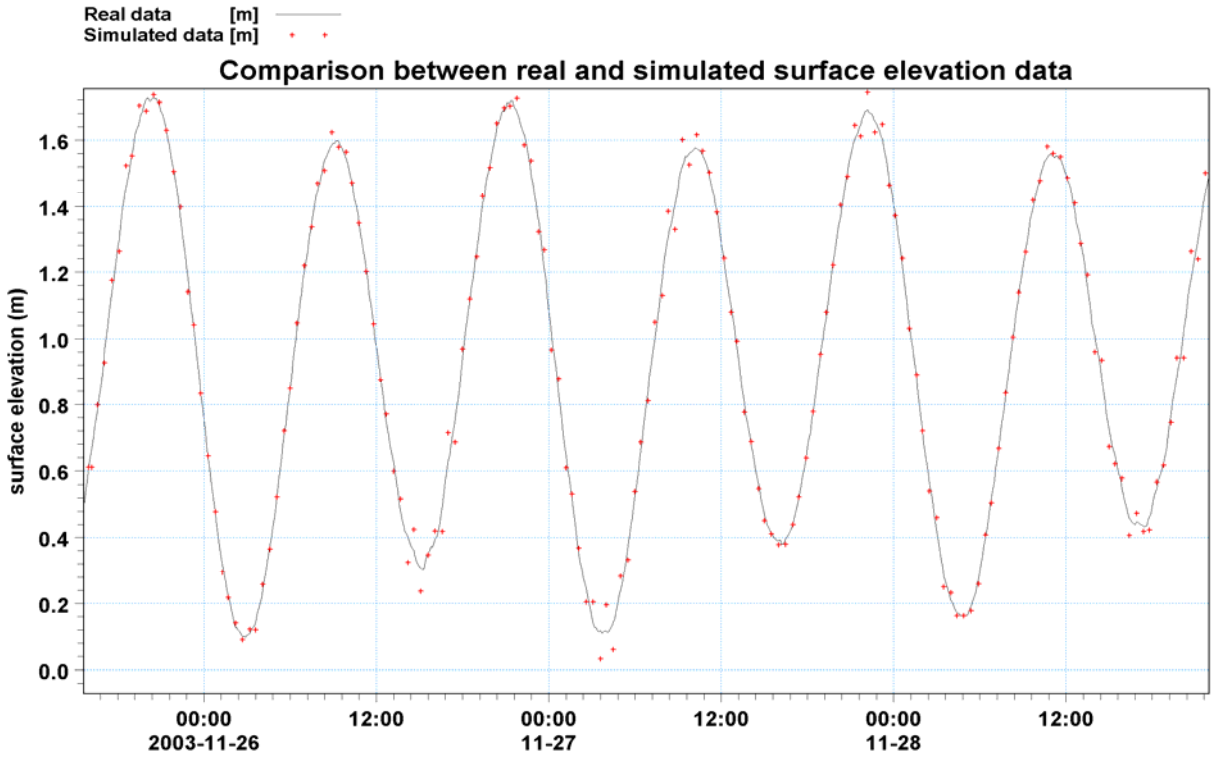

Figure 8: Calibration of the surface elevation

4.2 Current Speed

Figure 9 compares the ADV data collected in Fanga'uta with the simulated current speed.

While calibrating a 2D model, which simulates a depth averaged velocity, the use of ADV is not recommended since it only records data at one specific depth. The failure of the ADP instrument, which records current data over the water column, compromised the calibration of this model.

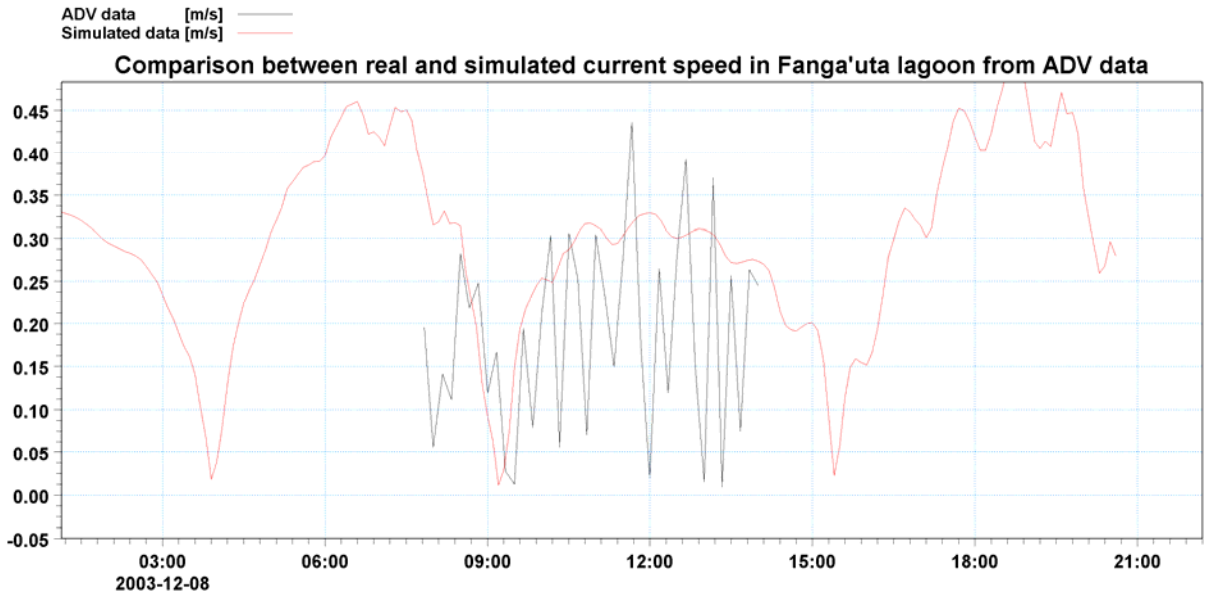

Figure 9: Current speed calibration

5. MODEL RESULTS

The model simulates a two-week period from 25 November to 10 December.

5.1 Global Circulation in Fanga'uta Lagoon

This embayment being highly sheltered, its water movement involves neither the wind- nor the wave-generated current. Only two main features are controlling the circulation: the current generated by the tides and two passes, i.e. the main lagoon entrance and the entrance of the Nuku'alofa branch.

Four distinct global circulation patterns were extracted: two during ebb and two during flood (Figures 10–13). These four patterns represent the interactions existing between the three system components of Fanga'uta lagoon: ocean, Pea sector and Vaini sector. Two of these are transitory patterns highlighting the differences between the large and deep pass from the ocean to Vaini (the Mu'a sector), and the shallow and narrow pass leading to Pea (the Nuku'alofa branch).

5.1.1 Ebb Regime

During ebb at the ocean side, the tidal current leads the water to be flushed out from Fanga'uta lagoon (Figure 10). This pattern takes place for five hours per tidal cycle averaged over a full lunar cycle.

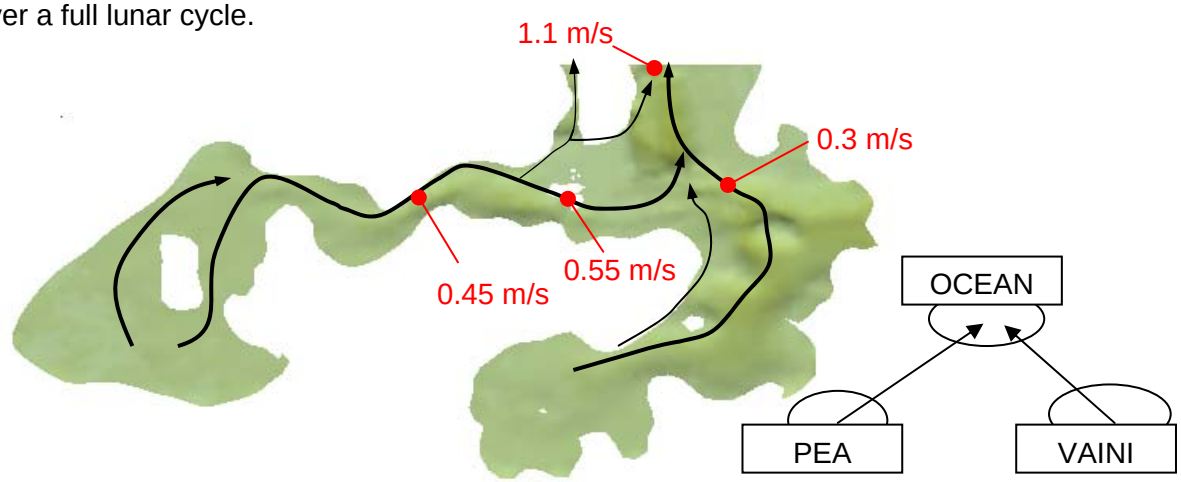

Figure 10: Ebb regime

The highest current speed occurs at the entrance and can reach, during the spring tides, more than 1.1 m/s. It can reach up to 0.3 m/s in the Mu'a sector, 0.55 m/s at the Nuku'alofa entrance and 0.45 m/s at the Nuku'alofa branch, next to the power station.

This regime begins when the surface elevation in the lagoon entrance is between 1.3 m and 1.5 m during the spring tides and between 1.2 m and 1.4 m during neap tides.

5.1.2 Flood Transitory Regime

As the surface elevation reaches a peak, the flood current leads the water to be flushed into the lagoon through the entrance mouth. Vaini being more open to the ocean than Pea, it responds much quicker to this change of current direction, which leads to a transitory regime. The flood current quickly controls the eastern branch, pushing the water from the ocean toward Vaini while the ebb current is still controlling the water motion in the Pea sector. The two branches are now connected as the Mu'a branch is partially filled by the Nuku'alofa branch water (Figure 11).

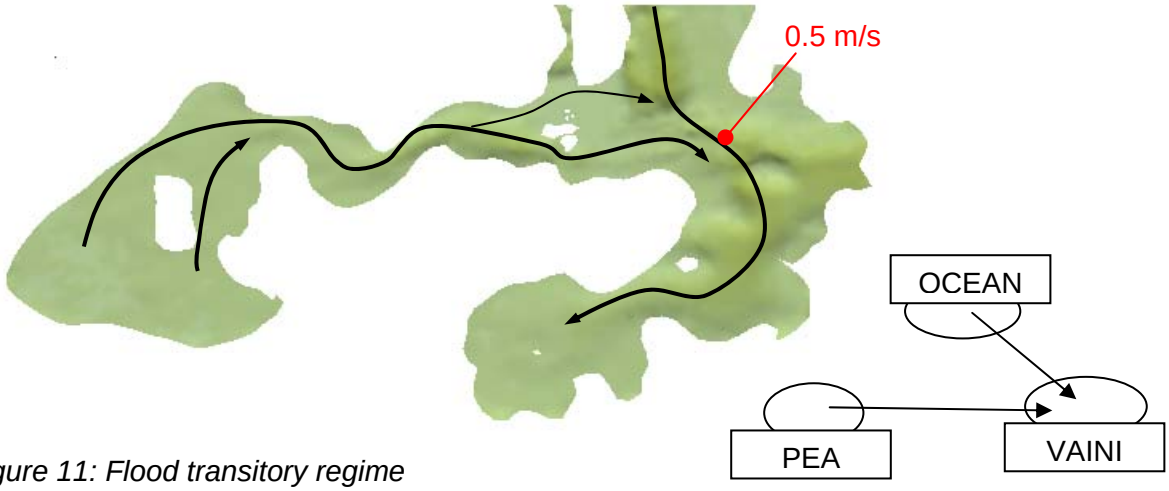

Figure 11: Flood transitory regime

The current speed can reach more than 0.5 m/s in the entrance of Mu'a sector. This regime takes place for 82 minutes per tidal cycle averaged over a full lunar cycle

During neap tide, this regime begins when the surface elevation at the lagoon entrance is between 0.5 m and 0.6 m. During spring tide, the flood transitory regime starts when the elevation in the lagoon entrance is between 0.2 m and 0.5 m.

5.1.3 Flood Regime

As the stress from the flood discharge overcomes the stress from the ebb discharge through the Nuku'alofa pass, the water circulation finds a more balanced regime, where the flood current now controls the water motion in both branches (Figure 12).

During spring tide, the current speed can be stronger than 1 m/s at the lagoon entrance, while it reaches a maximum of 0.5 m/s at Mu'a sector, a maximum of 0.7 m/s at Nuku'alofa pass and reaches a speed of 0.65 m/s next to the power station in Nuku'alofa branch.

This regime takes place for 3h40 per tide averaged over a lunar cycle.

The surface elevation in the lagoon entrance at the beginning of this regime is very steady over the spring to neap tide cycle, between 0.72 m and 0.84 m.

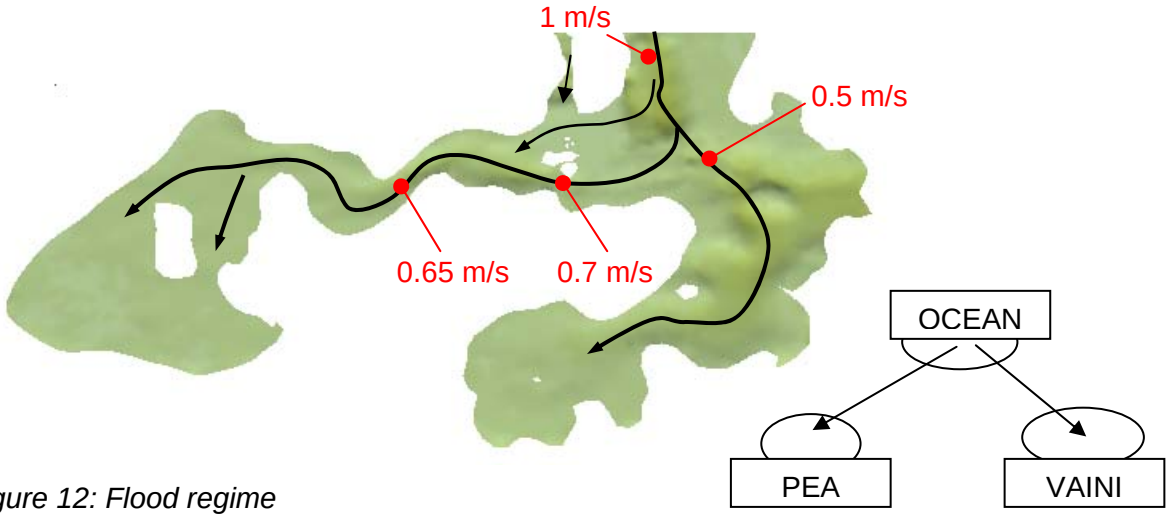

Figure 12: Flood regime

5.1.4 Ebb Transitory Regime

As the ebb current takes place in the ocean side, water in the entrance of Fanga'uta lagoon is flushed out. The late response of the current in Nuku'alofa branch to a change in ocean current leads to another transitory regime. The ebb current controls the water motion in the eastern branch while the flood current still controls the water motion in the western branch. As during the flood transitory regime, both branches are connected. However, in this regime, water is mixed in the western branch.

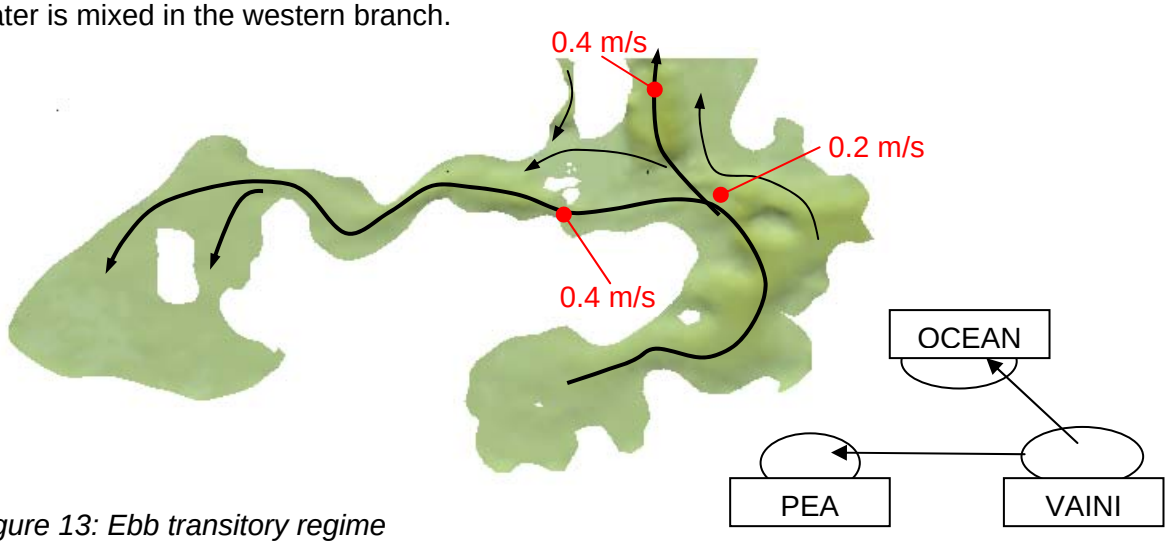

Figure 13: Ebb transitory regime

During the flood regime, the water speed reaches a maximum speed of 0.4 m/s at the entrance of Fanga'uta lagoon and Nuku'alofa branch but only 0.2 m/s at the entrance of Mu'a sector.

This regime takes place during 55 minutes per tide averaged over a lunar cycle.

5.2 Tidal Lag between Nuku'alofa Wharf, Pea and Vaini Sectors.

Since the two branches of Nuku'alofa have a different connection with the entrance mouth, a specific surface elevation delay and tidal range should occur in Pea and Vaini.

In this section, we compare surface elevation at the tide gauge, in Nuku'alofa wharf, in Pea and in Vaini.

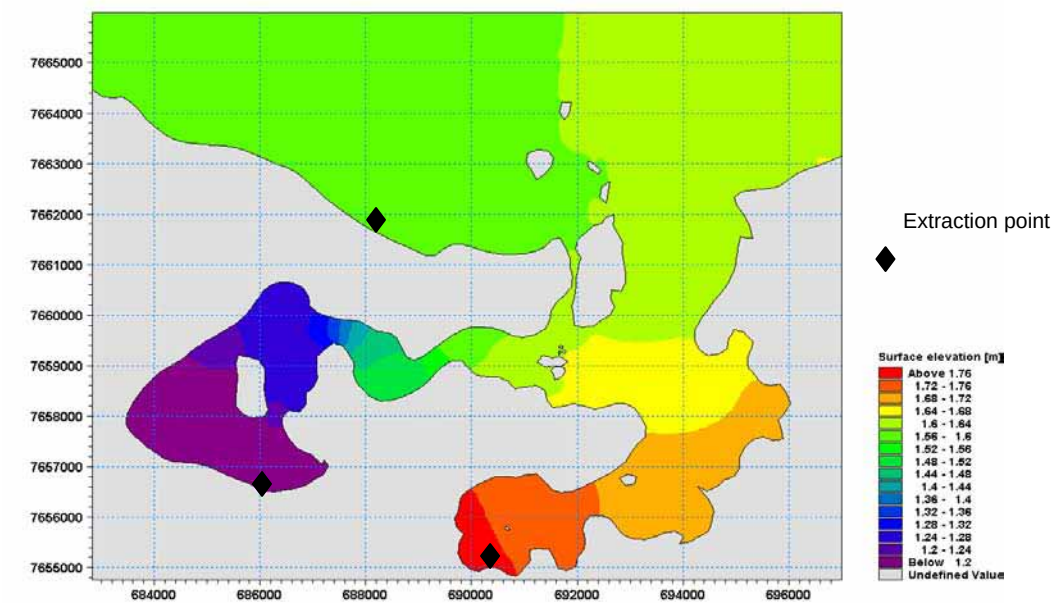

Figure 14: Extraction location for the tidal lag study

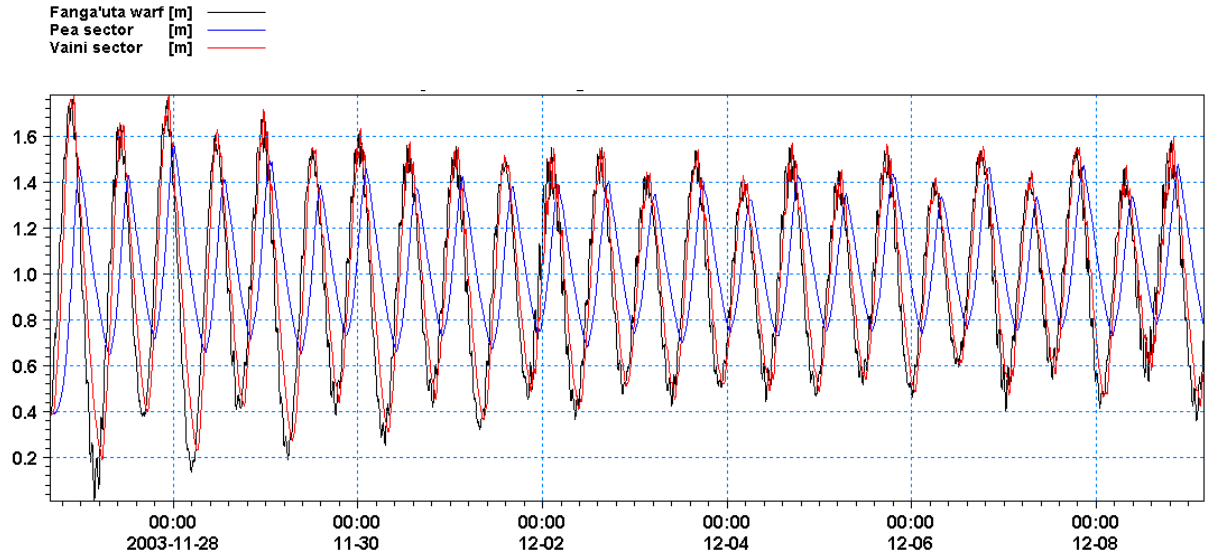

Figure 15: Tidal delay between Fanga'uta wharf, Pea and Vaini

As expected, according to the lagoon's three-dimensional shape, the tidal lag between Nuku'alofa wharf and Vaini is much shorter than with Pea.

At high tide, the tidal delay is steady and shorter than at low tide with a lag in Vaini of around 36 minutes (min) and around 2 hours (h) in Pea. In other words, both branches of the lagoon are filling much more quickly than they are emptied, which results from the temporary connection between the Mu'a sector and the Nuku'alofa branch: this is highlighted by the two secondary regimes: the flood and ebb transitory regimes.

At low tide, on average, the tidal lag in Vaini and Pea is 1 h 01 min and about 2 h 53 min, respectively.

However, at low tide the delay depends on the tidal range. Spring and neap tide periods are studied separately and tidal lag can be seen in more detailed in Table 1.

For both Vaini and Pea, the maximum lag is observed during spring and low tide, with 2 h and almost 4 h delay, respectively.

The two secondary water circulation regimes explain the height difference of the tidal waves between Nuku'alofa wharf, Vaini and Pea. During the flood transitory regime, Vaini is filled up with ocean water as well as from Pea, resulting in peaks in Vaini that are higher than at Nuku'alofa wharf.

During the ebb transitory regime, Pea is filled up with water coming from Vaini, resulting in a smaller height difference with Nuku'alofa wharf tidal peaks at high tide than at low tide.

5.3 Approximate Volume of Mixing Water

It is difficult to accurately estimate the volume of water exchanged between the eastern and western side of the lagoon, as unbalanced transitory circulation patterns occur while both sides are connected.

However, we assume that the water entering and leaving Pea sector during the ebb transitory regime and the flood transitory regime, respectively, is either coming from Mu'a sector or going to Mu'a. This assumption is in accord with the circulation patterns shown in Figures 11 and 13.

Table 1: Tidal lag in Fanga'uta lagoon compared to Nuku'alofa Wharf, where the tidal range is 1.7–0.93 m (SD = standard deviation).

		Vaini Sector		Pea Sector	
Max / min tidal range		1.6 m	0.93 m	0.9 m	0.58 m
Av. tidal lag at high tides ± SD.		36 min ± 6		118 min ± 8	
Max / min tidal lag at high tide		42 min	12 min	156 min	108 min
Av. tidal lag at low tide ± SD		61 min ± 22		173 min ± 29	
Spring	Av. tidal lag at low tide ± SD	103 min ± 22		216 min ± 21	
Spring	Max / min tidal lag at low tide	120 min	72 min	234 min	186 min
Neap	Av. tidal lag at low tide ± SD	52 min ± 4		146 min ± 13	
Neap	Max / min tidal lag at low tide	60 min	48 min	162 min	132 min
Av. height difference at high tide ± SD		0.013 m ± 0.03		–0.13 m ± 0.04	
Av. height difference at low tide ± SD		0.046 m ± 0.03		0.32 m ± 0.10	

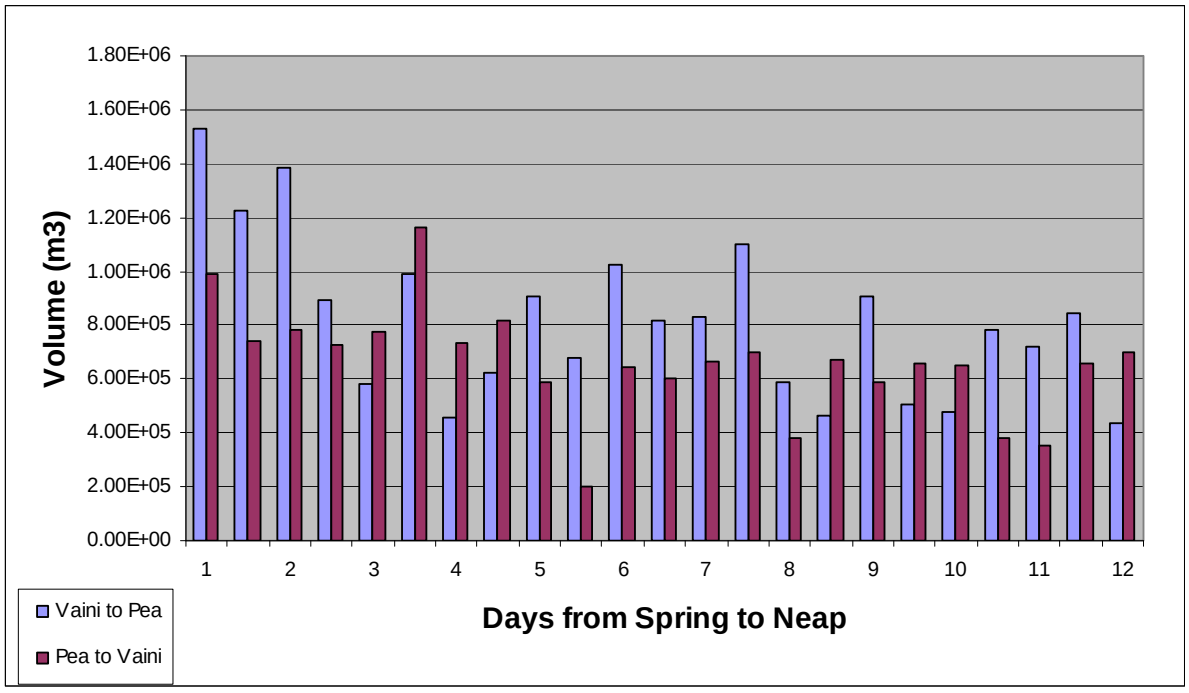

Figure 16: Volume of water exchanged between Vaini and Pea over a 12-day period

Over a lunar cycle the amount of Vaini water that reaches Pea, is around 18.7×10^6 m^3 or an average of 8.5×10^5 m^3 during each ebb transitory regime. Considering a surface elevation of 1.2 m constant along Nuku'alofa branch when the mixing occurs, the water coming from Vaini represents 3.3% of the water volume contained in Pea sector.

Over a lunar cycle the amount of Pea water reaching Vaini is around 15.2×10^6 m^3 or an average of 6.9×10^5 m^3 during each flood transitory regime. Considering a surface elevation of 0.5 m constant along Mu'a branch when the mixing occurs, the water coming from Pea represents 2.82% of the water volume contained in Pea sector.

The westward discharge is dominant since during the ebb transitory regime, the surface elevation is higher than during the flood transitory regime.

5.4 Water Renewal Time

Renewal time is defined as the lower bound of the turnover time, which is the average of the residence time over the whole lagoon. It can be calculated as the ratio of the lagoon volume to the daily volume flux entering or leaving the lagoon (Andrefouet et al. 2001).

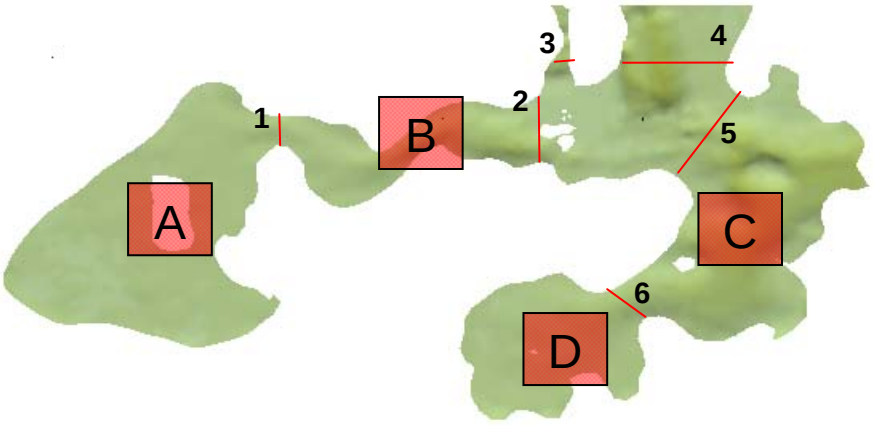

Figure 17: Section and area for water renewal time calculation

Discharge over a lunar cycle was extracted from the model in ten equidistant locations along every section (Figure 17). Calculation was carried out using a MATLAB routine and results are shown in Tables 2 and 3.

Table 2: Discharge across sections averaged over a tidal cycle

Section	Flushing in (m^3/s)	Flushing out (m^3/s)
1	328.26	240.68
2	456.53	364.29
3	107.23	90.221
4	1039	916.03
5	596.42	492.83
6	255.16	204.88

Table 3: Water renewal time results

Area	Flushing in (m^3/s)	Flushing out (m^3/s)	Flood %	Ebb %	V_e (m^3/day)	V_s (m^3/day)	V (m^3)	Renewal time R, using V_e (day)	Renewal time R, using V_s (day)
A	–328.26	240.68	42.7	58.3	1.211106	1.212105	8.586106	7.10	7.08
B	–697.21	692.55	42.7	58.3	2.572105	3.488105	1.403106	0.54	0.40
C	–801.3	747.99	45.9	54.1	3.177105	3.496105	7.369106	2.32	2.11
D	–255.16	204.88	45.9	54.1	1.012105	0.957105	1.637106	1.62	1.71
Lagoon	–1146.23	1006.251	45.9	54.1	45.45105	4.703105	1.376106	30.27	29.25

Renewal time only gives a rough idea of the lagoon's potential to clean itself. However, as it has been extensively used, some interesting comparisons could be made.

The water renewal time is higher in Pea than in Vaini, Mu'a or the Nuku'alofa branch. According to this figure, Pea is the most vulnerable part of the lagoon in case of a pollution scenario. The model estimates Fanga'uta lagoon's water renewal time to be between 29 to 30 days.

6. CONCLUSION

Using Mike21, a hydrodynamic model of Fanga'uta lagoon was developed. This model gives an understanding of the water circulation within the lagoon. Four main circulation regimes were extracted highlighting the tide-induced current dominancy: two primary regimes, the ebb and the flood regime and two secondary regimes, the ebb transitory and flood transitory regime. The secondary regimes reveal some interesting features, where the eastern and western branches of the channel are connected.

From this observation, we can quantify the amount of water exchanged between the two branches of the lagoon. During each tidal cycle, 3.3% of the eastern branch's water body comes from the western branch of the lagoon, while 2.8% of the western branch's water body comes from the eastern branch.

Tidal lags between Nuku'alofa wharf, Pea and Vaini were looked at. The three-dimensional shape of the lagoon, with a shallow and narrow entrance towards Nuku'alofa branch and a wider and deeper entrance to Mu'a sector, strongly influences the tidal lag within the lagoon. This results in a delay between Nuku'alofa wharf and Pea much longer than between Nuku'alofa wharf and Vaini.

Water renewal time calculations showed a 30 days' water renewal time. This relatively long water residence time for such a small lagoon area is an important detail for future water quality studies of Fanga'uta lagoon.

With more data being collected, this model could easily be improved and used as a management tool to address any coastal management project related to Fanga'uta lagoon. A recent upgrade of the software from 2D to 3D modeling will offer even better answers.

7. REFERENCES

Andrefouet, S. Pages, J. and Tartanville, B. 2001: Water renewal time for classification of atoll lagoons in the Tuamotu Archipelago, *Coral reefs 20(4):* 399–408.

Barstow, S and Haug, O, 1994: The wave climate of the Kingdom of Tonga, *SOPAC technical report 201.*

DHI 2004: Mike 21 Reference Manual

APPENDICES

Appendix 1: Water Circulation in Tongatapu Lagoon

Following a request from SPC to help them understand the local distribution and recruitment pattern of trochus shells on reefs, a model of Tongatapu lagoon was developed using data available. There were too few data for reaching a satisfactory current speed calibration: wave data, current data and depth along the reefs would be required.

However, a set of SOPAC data from a previous study provided current data from ADP deployment, seasonal wave data, bathymetry data, wind and surface elevation data. The model shows fairly well the relative importance of tide-, wind- and wave-induced current in the water circulation.

Although the model cannot be used for detailed hydrodynamic study, this simulation can provide a preliminary understanding of the overall water circulation.

A1.1 Wave Climate

The wave climate is extracted from Barstow and Haug (1994). This report gives a monthly variation of various wave parameters measured by a Waverider.

Unlike winds, the waves are seasonal, with significant wave heights averaging about 2.2 m in November to March and increasing to about 2.4 m in May to September. The distribution of the peak wave period, T_p, is slightly greater than 10 seconds. The swell is coming from the south, mainly southwest.

Figure A1.1 shows the predicted wave diffraction from a constant wave field coming towards Tongatapu from the southwest, at 220 degrees.

The radiation stress (Sxx,Sxy,Syy) was extracted from this model to introduce wave-induced flow in the hydrodynamic model.

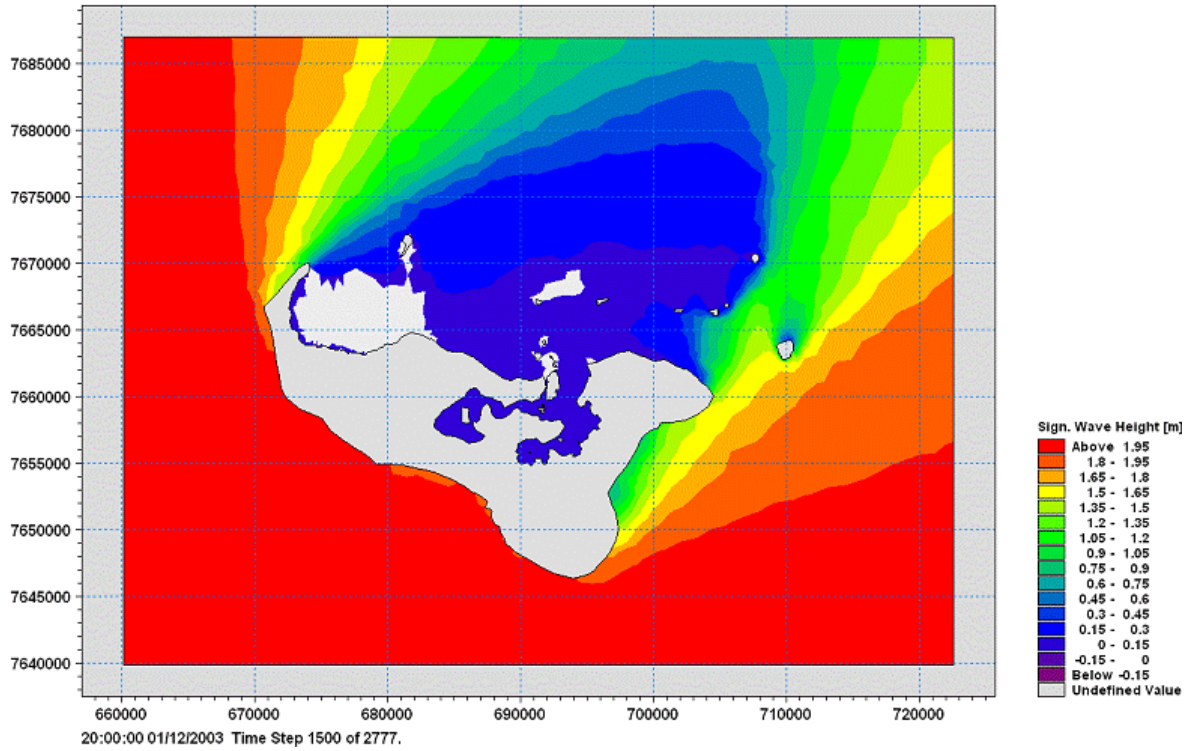

Figure A1.1: Wave diffraction derived from the model (using offshore wave data from Barstow & Haug 1994)

A1.2 Calibration

The surface elevation and current speed from the model respectively are compared with the tide gauge data located at the Nuku'alofa wharf and the ADP data, deployed on the western reef (Figure A1.2)

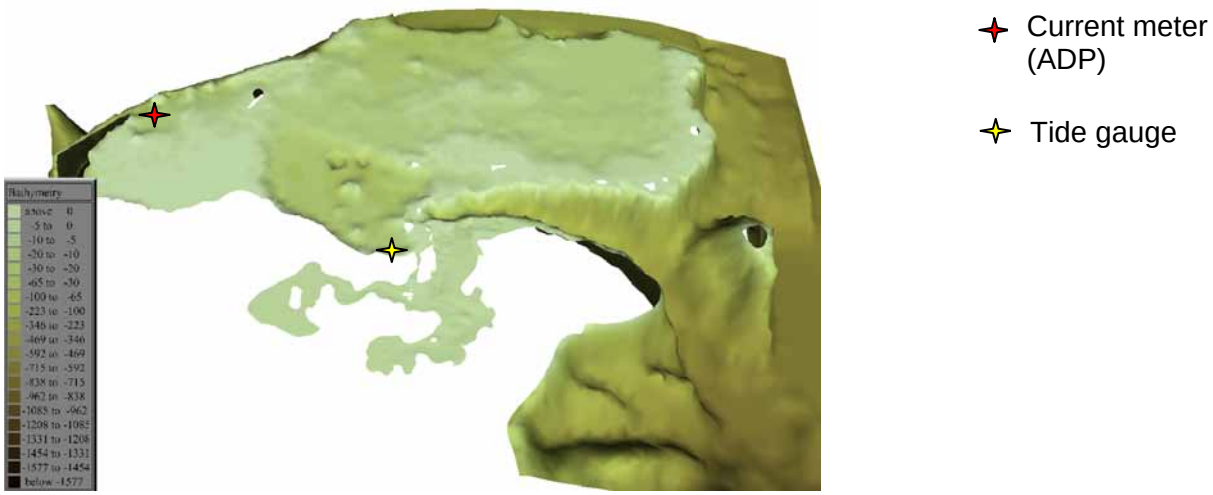

Figure A1.2: Acoustic Doppler profiler (ADP) and tidal gauge locations

A1.2.1 Surface Elevation.

The surface elevation in the model matches the tide gauge data well. The tidal fluctuation is well represented by the model (Figure A1.3).

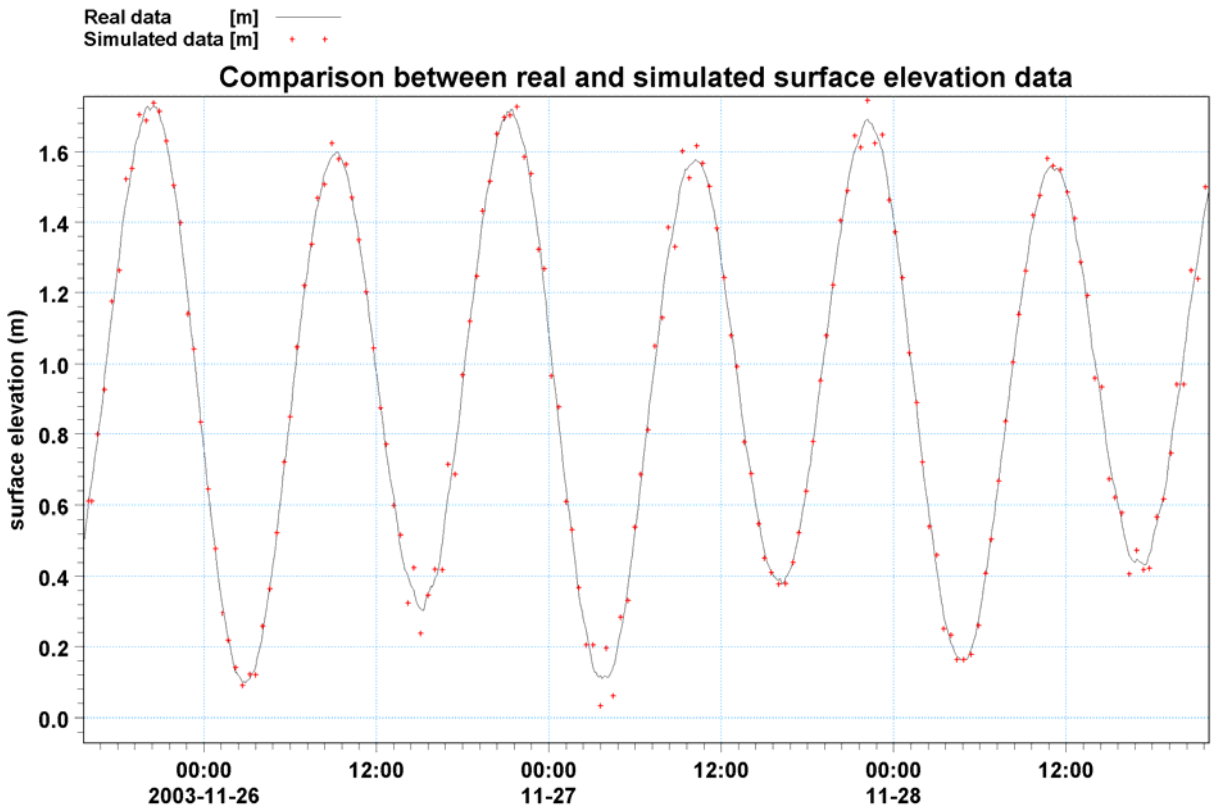

Figure A1.3: Surface elevation records and model data

A1.2.2 Current Speed

Satisfactory calibration could not be achieved (Figure1.4). At this location, the water motion is partly controlled by the wave-induced current as well as the surrounding reefs system. Reef depth had to be estimated and wave data were highly averaged.

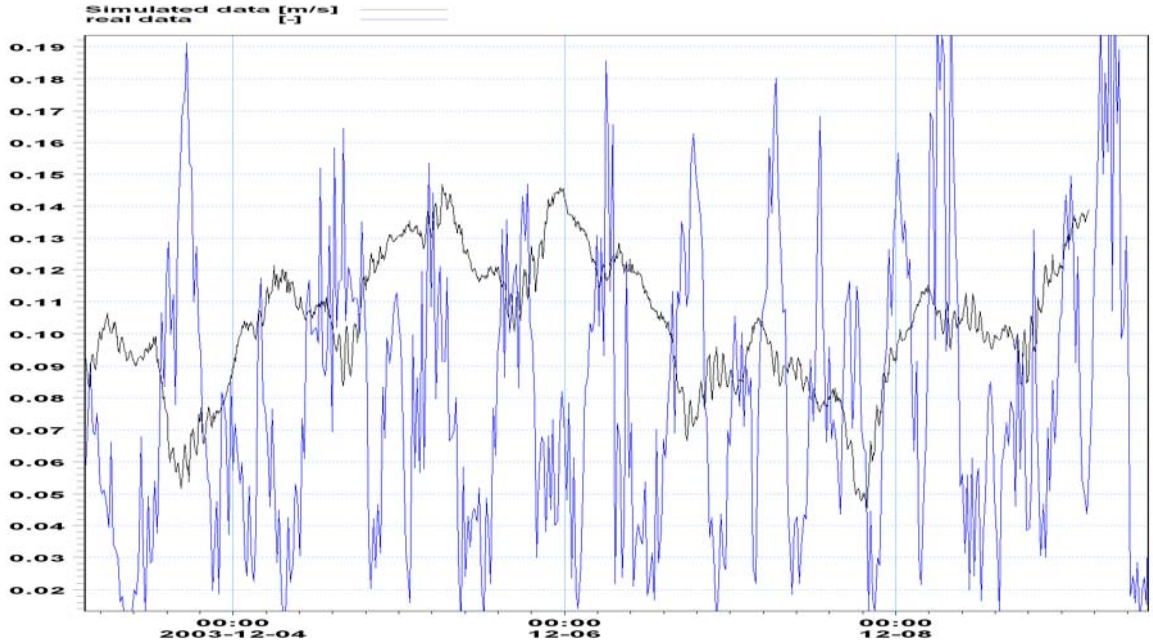

Figure A1.4: Comparison between current speeds collected and simulated

The result of this simulation cannot be considered for detailed hydrodynamic study; however it gives us an understanding of the global water motion.

A1.4 Circulation Patterns in Tongatapu Lagoon

Three currents are involved in the Tongatapu water circulation: tide-, wind- and wave-induced current.

The tidal current is dominant at spring tide during flood while only slight involvements of wave- and wind-induced current are observed. At high tide, the lagoon is filled up from all sides (Figure A1.5).

During ebb, the tidal current pushes the water out of the lagoon (Figure A1.6).

However, the water is flushed in the lagoon across the southeast corner of the atoll rim, as the wave-induced flux competes with the ebb current.

Inside the lagoon, the westward current is generated from the easterly wind.

At neap tides, the tidal current decreases and the circulation in the lagoon is mainly controlled by the easterly wind (Figures A1.7 and A1.8).

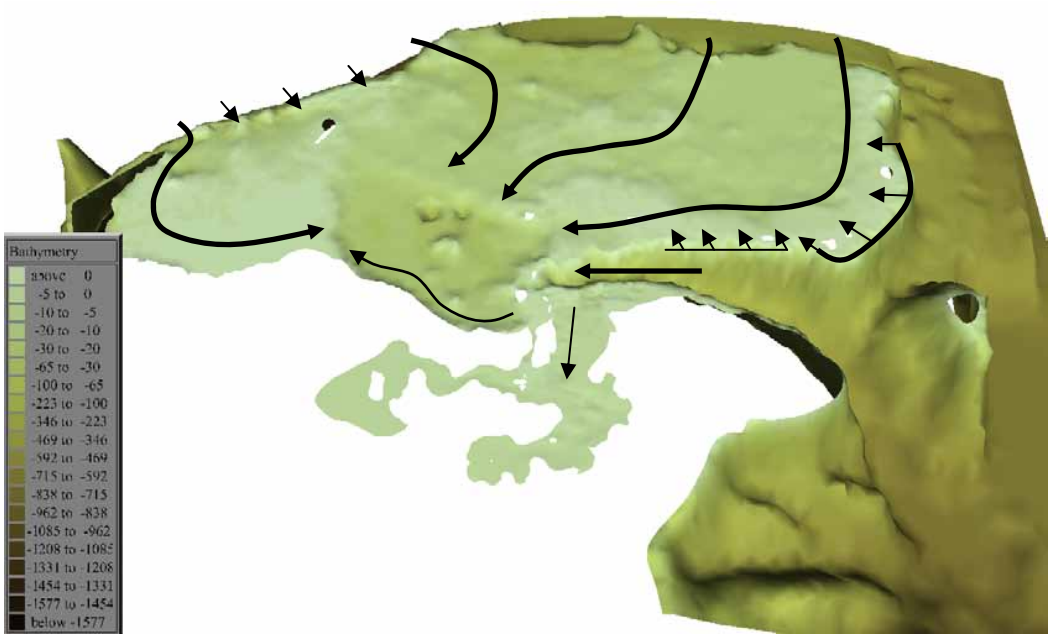

Figure A1.5: Circulation pattern at spring tide during flood

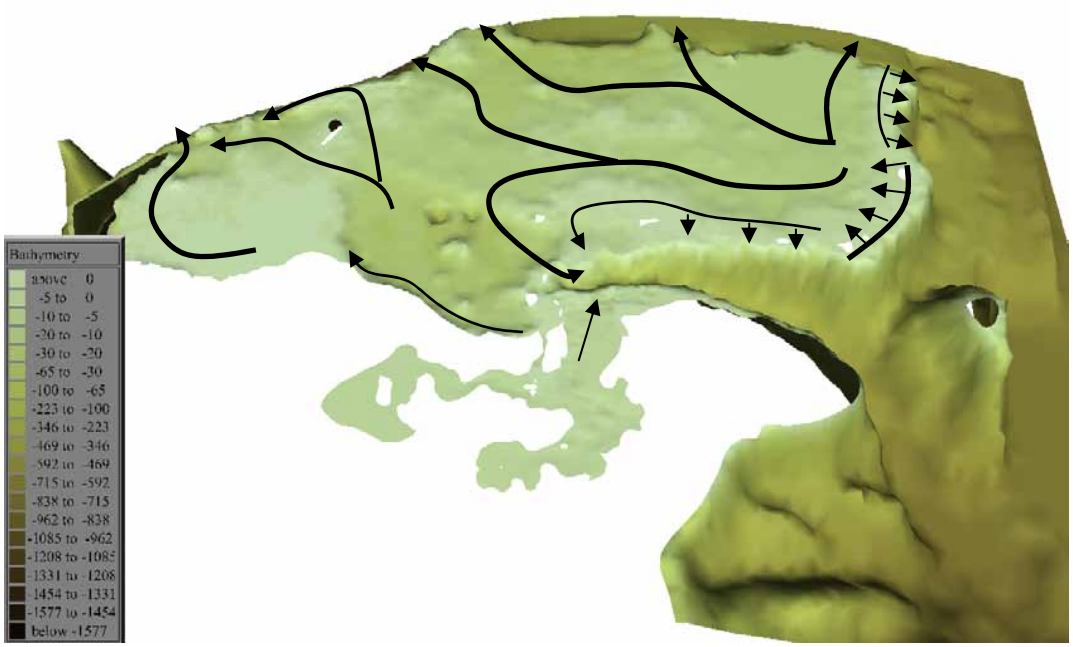

Figure A1.6: Circulation at spring tide during ebb

A1.5 Conclusion

It is not possible to undertake any detailed study from this model since it is only calibrated against the tide gauge data. Yet an understanding of the global circulation pattern during normal weather condition can be reached. During spring tides, tidal current controls the water motion, except in the southeast corner of the rim where the wave current permanently pushes water into the lagoon. As the tidal range decreases, wind-induced current quickly plays a greater role and induces a westward movement in the lagoon.

In order to complete this work, acoustic Doppler profilers (ADP) should be deployed on the eastern side and the central part of the lagoon for collecting current and wave data. Also bathymetry data are required from along the western and eastern reef.

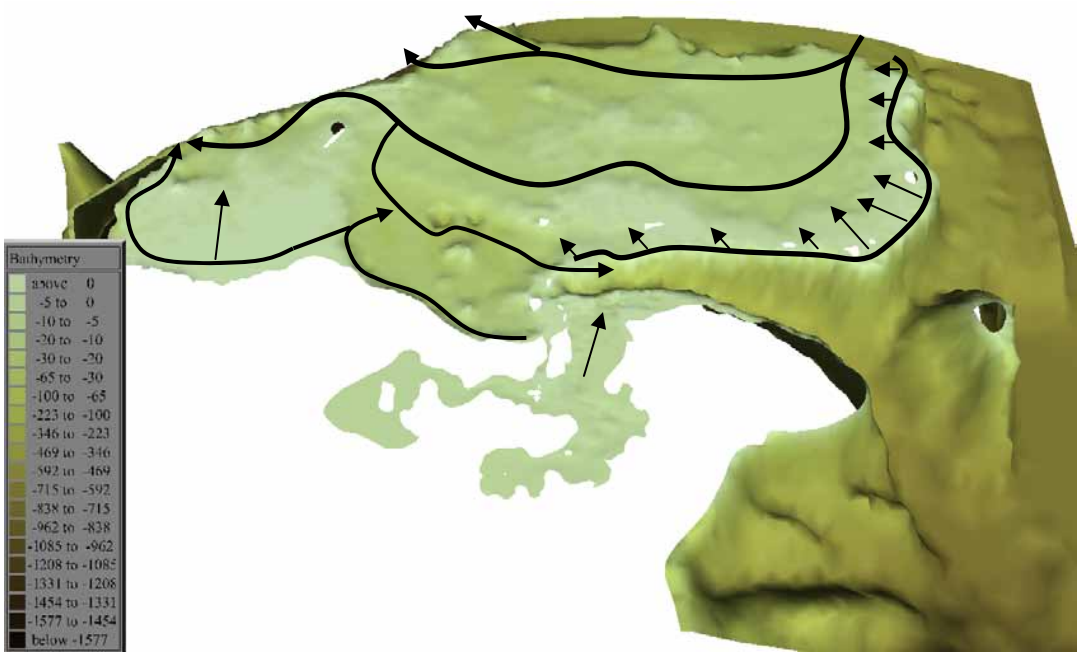

Figure A1.7: Circulation at the neap tide during ebb

Figure A1.8: Circulation pattern at neap tide during flood

Appendix 2: Water Quality Data Collection and Results

In the sea, oxygen levels change significantly from day to night. Photosynthesis by microscopic plants during the day releases oxygen into the water column, so oxygen level increases. At night, photosynthesis stops in the absence of sunlight. Oxygen is no longer produced and its level drops while it is consumed by other organism. In polluted water, excess of nutrients can lead to extremely low level of oxygen at night, which can be stressful and sometimes deadly for aquatic life. Hence oxygen production is a key indicator of the lagoon's health.

Water quality data was collected in the eastern branch of Fanga'uta lagoon, in the eastern branch to quantify the oxygen production. From a water renewal time point of view, the eastern branch, especially Pea is the most vulnerable area of Fanga'uta lagoon.

Dissolved oxygen (DO) data were collected in six locations Figure A2.1), at different times of the day: 1600, 2200, 0400, 1200 hours. Respiration, net and gross production of oxygen were calculated.

Respiration is the quantity of oxygen consumed by the aquatic life. Gross production shows the total oxygen produced (i.e. photosynthesis or water-air interface) and net production is the resulting increase of oxygen in the water column after respiration.

Results from the survey (Figure A2.2) show an oxygen production greater than respiration at all sites, oxygen released in the water column is enough to ensure the well-being of the lagoon aquatic life.

Very low respiration and oxygen production rates were observed at sites 2 and 3, due to run-off from the power plant. This could lead to unbalance the ecology of Fanga'uta lagoon.

While dissolved oxygen is a useful indicator for lagoon health, other data, such as coliform and nutrients, should be looked at to reach a definitive conclusion.

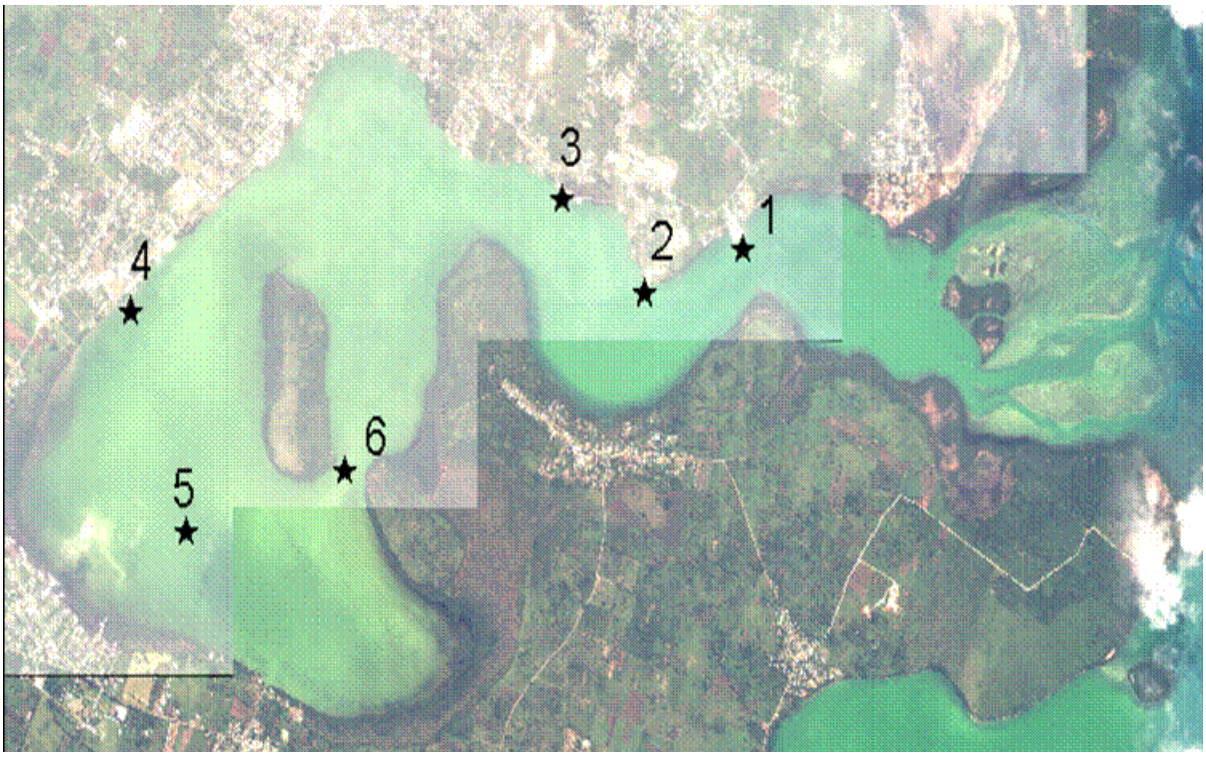

Figure A2.1: Location of sampling points for the water quality data collection

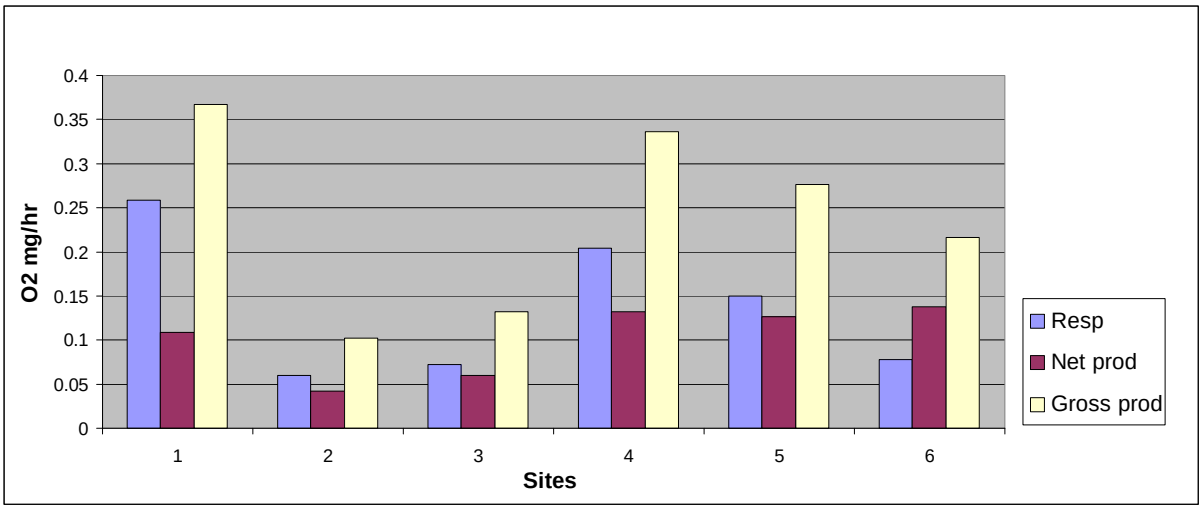

Figure A2.2: Results of water quality data analyses: Gross production, Net production and Respiration are lowest near the power plant